

Calculation and design of a Ni-like Eu soft-x-ray laser

S. Maxon

University of California, Lawrence Livermore National Laboratory, Livermore, California 94550

P. Hagelstein

Research Laboratory of Electronics, Massachusetts Institute of Technology, Cambridge, Massachusetts 02139

B. MacGowan, R. London, M. Rosen, J. Scofield, S. Dalhed, and M. Chen

University of California, Lawrence Livermore National Laboratory, Livermore, California 94550

(Received 24 August 1987)

Numerical calculations of laser-irradiated EuF_2 targets predict gain coefficients of $0.3\text{--}1.6\text{ cm}^{-1}$ on several $4d\text{--}4p$ Ni-like Eu lines from 66 to 104.5 \AA . Dielectronic recombination is important both in determining the ionization balance and in populating the $J = 1, 2$ $4d$ excited states. Targets which are optimized for $0\text{--}1$ gain show significantly less effect due to trapping on the $0\text{--}1$ line than on the $2\text{--}1$ line.

Clear evidence for amplification in the far ultraviolet or soft-x-ray region has been published in recent years.^{1–5} The gains and wavelengths measured are 5.5 cm^{-1} at 206.3 and 209.6 \AA ,^{1,2} 8 cm^{-1} at 182 \AA ,³ and 6.5 cm^{-1} at 182 \AA .⁴ Recently, a gain coefficient of 3 cm^{-1} has been obtained in H-like F at 81 \AA (Ref. 5), and a gain coefficient of 2 cm^{-1} for a $0\text{--}1$ line has been measured in Ne-like Cu.⁶

In order to obtain a soft-x-ray laser in the $40\text{--}100\text{ \AA}$ range, we have suggested working with Ni-like ions of the rare earth elements.^{7,8} This paper on theory together with the experimental results recently published⁹ clearly demonstrate lasing on two $0\text{--}1$ $4p\text{--}4d$ lines of Ni-like Eu with measured wavelengths of 65.83 and 71.00 \AA . The calculations described in this paper were the basis for the design of the targets used in the experimental study.

As discussed later, the $J = 0$ states are populated by monopole excitation¹⁰ from the ground state, while the $J = 1, 2$ states receive a large contribution to their populations through dielectronic recombination from the Co-like ground state. A most significant outcome of the Ni-like experimental work is the fact that the $0\text{--}1$ laser lines are seen on every shot with their full calculated gain, as will be presented in this paper. This is in direct contrast with the Ne-like Se experiments^{1,2} in which the $0\text{--}1$ lines were not identified.¹¹ While Ne-like Mo has produced a $0\text{--}1$ line at 106 \AA with a gain of 2 cm^{-1} (Ref. 12) and at longer target lengths the Se $0\text{--}1$ line has been observed to have gain,¹³ attempts to resolve the $0\text{--}1$ discrepancy have not fully succeeded to date. It should be noted that in Ni-like systems the $0\text{--}1$ transitions scale more rapidly than other transitions with atomic number (Z) to shorter wavelengths.

Another important point of this work is the fact that trapping¹⁴ is important in the Ni-like system. There is a much larger oscillator strength for the $3d\text{--}4p$ Ni-like transition than for the $2p\text{--}3s$ Ne-like transition because of the lower principal quantum numbers and lower angular momentum in the Ne-like case. The calculated ratio of

these oscillator strengths is 6. The effect of trapping on the gain coefficients is shown later in this article.

We now introduce Fig. 1, where a simplified energy-level diagram as well as rates connecting some of the levels for Ni-like Eu are shown. Laser transitions ($4p\text{--}4d$) are indicated as well as the characteristic x rays which are used to identify the presence of these ions. The position of the $(3d_{3/2}4d_{3/2})_{J=0}$ state is difficult to calculate due to mixing with the 1S_0 ground state. The energy has been determined through the use of the multi-configurational, relativistic Hartree-Fock method,¹⁵ including orbital relaxation effects. The remaining levels and decay rates were obtained from a superposition of configuration Hartree-Fock calculations.

The $4\text{--}4$ spectra of Cu-like and Zn-like ions of the rare earths have been reported.¹⁶ This work has been the basis of our wavelength calibration and our comparison of theoretical with experimental wavelengths.

Our x-ray laser experiment uses the exploding foil technique.² The expansion of our target upon irradiation in the two-beam chamber of the NOVA laser facility of the Lawrence Livermore National Laboratory is calculated using the Lagrangian hydrodynamic code LASNEX.¹⁷ Then the time-dependent plasma conditions and spectra for different zones, along with the atomic model, are used as input for the kinetic code XRASER.¹⁸

The Ni-like model includes the M -shell and N -shell state in detail and Rydberg states up to $n = 10$ (137 levels total). The $3\text{--}4$ collisional excitation rates were computed in the relativistic distorted wave approximation,¹⁹ and the $4\text{--}4$ collisional excitation rates are calculated in the classical path model. In the Cu-like sequence, the $n = 4$ and $n = 5$ states are treated in detail using atomic data from Ref. 20. Hydrogenic Rydberg states up to $n = 10$ are included. The other sequences were modeled using largely hydrogenic physics, except for the Zn-like sequence, which has detailed $n = 4$ levels.

The dielectronic recombination coefficients for the Ni-like to Cu-like sequence were calculated in the quantum-

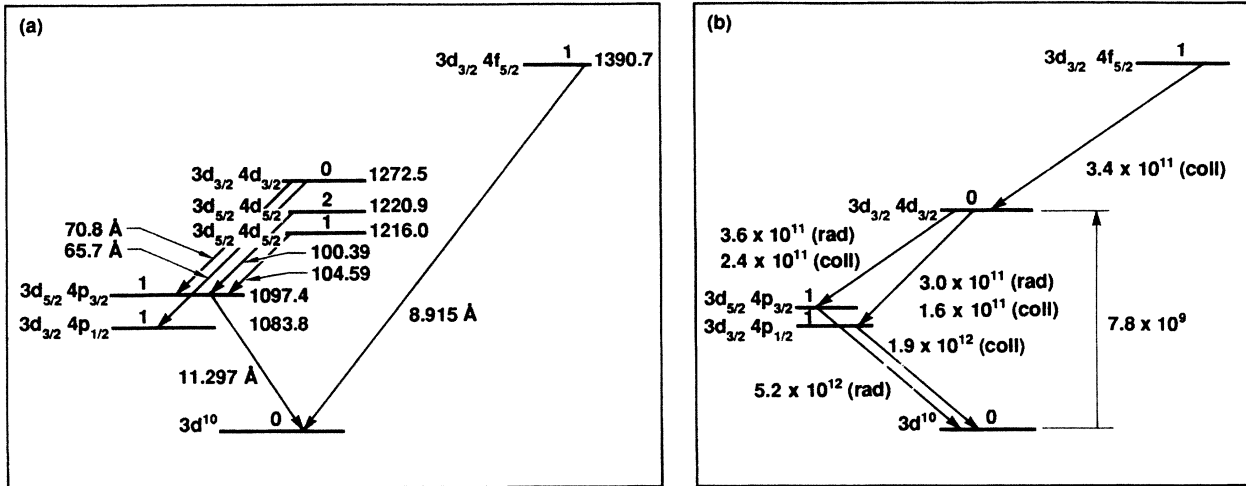


FIG. 1. Simplified energy-level diagrams for Ni-like Eu. Energies are given in eV. The properties of the levels are shown in (a) and the collisional and radiative rates pertaining to the laser transition $(3d_{5/2}4p_{3/2})_1-(3d_{3/2}4d_{3/2})_0$ at $n_e = 3 \times 10^{20} \text{ cm}^{-3}$ and $T_e = 700 \text{ eV}$ are shown in (b).

defect approximation based on the relativistic distorted wave results of Ref. 19. The resulting total recombination rate coefficients agree with the results of Ref. 21 to within about 20%. The data for the other sequence are obtained by casting the data in the \bar{f} and $\bar{\lambda}$ model described in Ref. 22. This approach to modeling dielectronic recombination in collisional n - n laser schemes is appropriate for obtaining both the effects of dielectronic recombination on $n = 4$ population, and for obtaining the reduction of recombination coefficient due to density effects to lowest order, as described in Ref. 23.

Before dielectronic recombination was available in the data file, its effect was simulated by a rate coefficient of $1 \times 10^{-10} \text{ cm}^3/\text{s}^{21}$ connecting the ground states of succes-

sive ions. Using the data file including dielectronic recombination and without these ground-state-to-ground-state coefficients caused an increase in \bar{Z} by almost one unit.

Determining the appropriate value of the ground-state-to-ground-state coefficient resulted in a reduction in the dielectronic recombination rate from $1 \times 10^{-10} \text{ cm}^3/\text{s}$ to $3 \times 10^{-11} \text{ cm}^3/\text{s}$, due to density effects. This reduction in the recombination rate from Co-like to Ni-like Eu is 20% larger than the reduction in the rate from F-like to Ni-like Se.²³

As we mention later, dielectronic recombination from the Co-like ground state (followed by decay) is a major population mechanism for the $(5/2, 5/2)_2$ level.

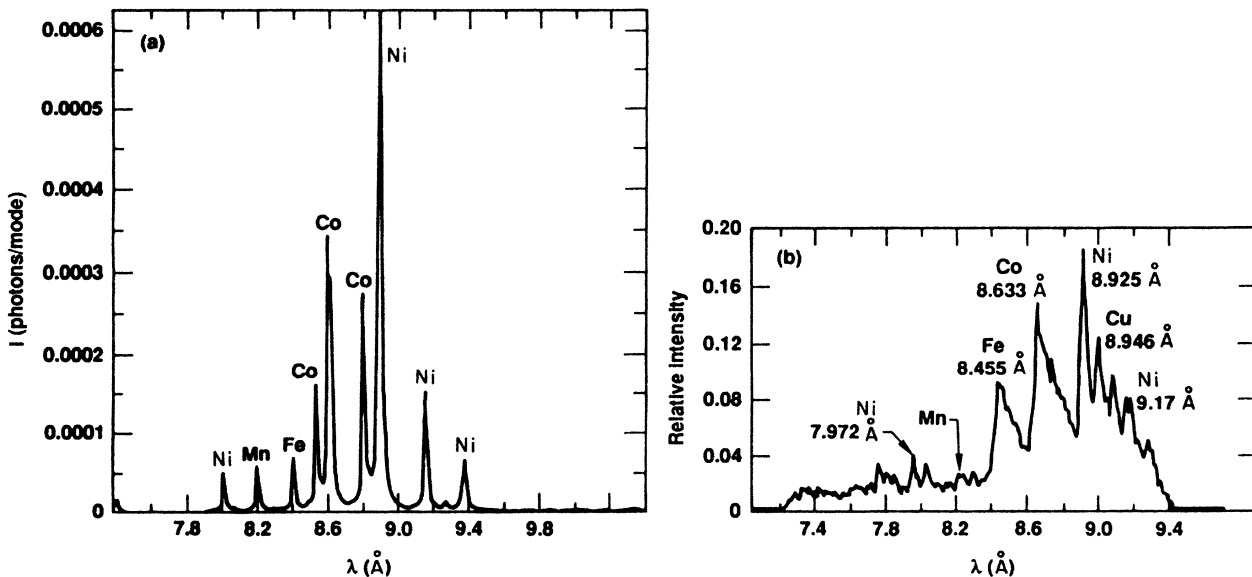


FIG. 2. 4-3 spectrum for the $60 \mu\text{g}/\text{cm}^2$ target at $t = 0.7 \text{ ns}$ as (a) calculated with instrument broadening of 3.0 eV and (b) measured.

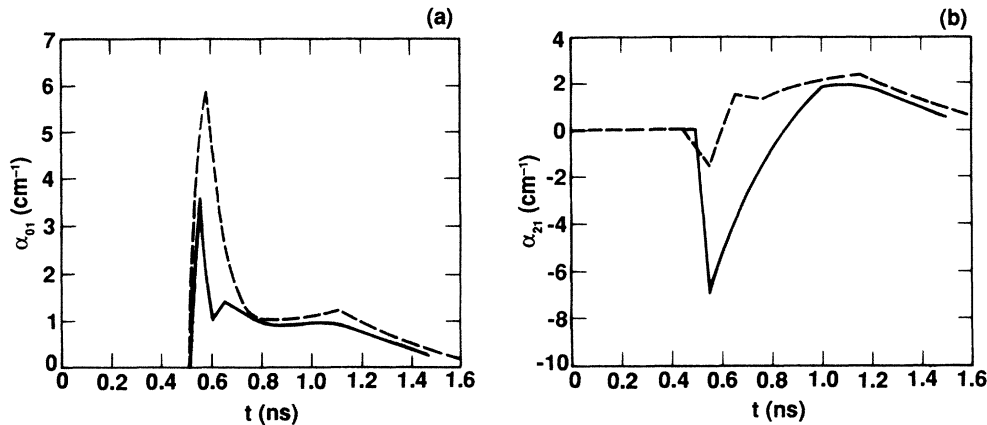


FIG. 3. Gain curves for the case with irradiance 5.7×10^{13} W/cm², where the 0-1 line at 71 Å is plotted in (a) and the 2-1 line at 100.39 Å is plotted in (b). The solid lines are calculations with trapping and the dotted lines are results for calculations with no trapping.

The simulation of two EuF₂ targets,⁹ 60 and 100 μg/cm², are discussed in this work. The oxidation kinetics and description of the fabrication of these targets can be found in Ref. 24. If we arbitrarily set the peak of the input pulse with 1 ns full width at half maximum (FWHM) to be at 1.0 ns, then for the 60 μg/cm² target the laser burns through the foil at ~600 ps. The electron-density profile at the peak of the input pulse resembles a Gaussian with a FWHM of 232 μm and a peak value of 3.4×10^{20} cm⁻³. This should insure good beam propagation down the length of the target without severe refraction. The electron temperature in this region ranges from 650–700 eV.

To investigate the degree of ionization, the 3*d*-4*f* lines are measured, spatially integrated but time dependent. Identifications of spectral lines from Ni-like, Co-like, and Fe-like Eu have recently been published.²⁵

Since our atomic data file does not treat detailed Co lines, we can only compare Co to Ni emission qualitatively. In Fig. 2 the calculated and measured 4-3 spectrum for the 60 μg target (plotted at a time corresponding to the peak of the x-ray pulse) indicate that we are predicting the ion abundance correctly. For the 100 μg target, the 4-3 spectrum shows that the Co emission is clearly larger than the Ni emission, a feature which also holds for the calculated spectrum. The ionic abundances for the 60 μg/cm² target calculated at $t = 1$ ns are 18% Mn-like, 25% Fe-like, 32% Co-like, and 16% Ni-like.

The dominant contribution to the level $(3d_{5/2}4d_{5/2})_2$ is recombination from the Co-like ground state into high-lying Ni-like Rydberg states ($n = 5, 6$), which then populate the $J = 2, 1$ levels both directly and indirectly. Higher-lying Rydberg states are collisionally ionized. On the other hand, the only mechanism populating level $(3d_{3/2}4d_{3/2})_0$ is the monopole transition from the ground state. In Fig. 1(b) we show the rates which are relevant for populating states $(3d_{3/2}4d_{3/2})_0$.

In Figure 3 we show the simulated trapped and untrapped gains near the center of the foil for the 0-1 line at 71 Å and the 2-1 line at 100.39 Å. The untrapped case is calculated in XRASER by neglecting radiation transfer for

the Ni-like resonance lines.

The time and space averaged gains (including refraction) are obtained by comparing intensities calculated by SPECTRE (Ref. 26) at $L = 1.67$ and 3.48 cm. The average gains for the 60 μg, 5.7×10^{13} W/cm² calculation can be found in Table I. Comparing these results with experiment,⁹ we find that the gain is in agreement for the 0-1 lines at 71 Å and 65.83 Å, but we predict gains 0(1) for the 2-1 and 1-1 lines at 100.39 and 104.5 Å, where linear growth is measured.⁹

To optimize the 0-1 yield, consider the 60-μg problem discussed above but with an irradiation of 3.6×10^{13} W/cm². The temperature is now 480 eV, and the Ni-like fraction is 45% instead of the previous 16% at $t = 1$ ns (peak of the input pulse). In Fig. 4 the trapped and untrapped 0-1 and 2-1 lines are plotted. Comparing Figs. 4(a) and 3(a) we see larger gain for $t > 0.64$ ns, when refraction is no longer a problem, due to the larger Ni-like abundance.

Next compare the trapped and untrapped gains in Fig. 4. The most dramatic effect is on the 2-1 line. The gain becomes positive at 0.8 ns in the trapped case and 0.6 ns in the untrapped case. The average gain in the trapped (untrapped) case is 0.6 cm⁻¹ (2.6 cm⁻¹). For the 0-1 line, the average gain is 1.9 cm⁻¹ (4 cm⁻¹) in the trapped (untrapped) case. Therefore, as we optimize the 0-1 emission, the 2-1 emission decreases and the 2-1 gain becomes more sensitive to trapping.

A 28% decrease in the population of the $J = 2$ state or a corresponding 28% increase in the $J = 1$ state would

TABLE I. Gains for the 60 and 100 μg/cm² targets.

Line	60 μg gain (cm ⁻¹)	100 μg gain (cm ⁻¹)
$(5/2, 3/2)_1 - (3/2, 3/2)_0$	1.2	0.7
$(3/2, 1/2)_1 - (3/2, 3/2)_0$	0.36	0.3
$(5/2, 3/2)_1 - (5/2, 5/2)_2$	1.4	1.15
$(5/2, 3/2)_1 - (5/2, 5/2)_1$	1.0	

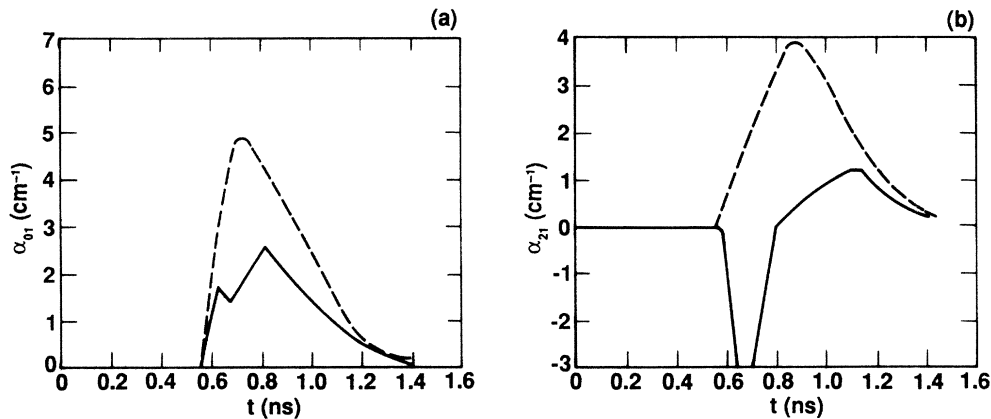


FIG. 4. Time-dependent gain curves for the case with irradiance $3.6 \times 10^{13} \text{ W/cm}^2$.

reduce the 2-1 gain to zero without significantly reducing the 0-1 gain. Therefore an improvement in either our treatment of trapping and/or dielectronic recombination calculations may explain the 2-1 discrepancy.

Summarizing, we have carried out numerical calculations on exploding foil experiments obtaining essential agreement with 0-1 lasing transitions in Ni-like Eu. Experiment⁹ shows linear growth for the 2-1 and 1-1 transitions and we are currently investigating this discrepancy with theory. We have found that it is necessary to include dielectronic recombination both from the point of view of ionization balance and kinetics. We also find that trapping makes a significant difference in the gain coefficient. The persistence of the 0-1 lines at 66 and 71

Å with gain $\sim 1 \text{ cm}^{-1}$ is indeed encouraging and suggests that work is needed to increase the number of gain lengths, proceeding towards W and Re, for which the equivalent 0-1 lines are at 43.11 and 40.76 Å.

We gratefully acknowledge discussions with M. Eckert, M. Klapisch, J. Seely, A. Zigler, and W. Hodge concerning spectroscopy. We thank B. Shore and J. Trebes for discussions, and L. Minner, R. Minner, and M. Runyan for code support. The support and encouragement of J. Lindl and J. Nuckolls are acknowledged. This work was performed under the auspices of the U.S. Department of Energy by the Lawrence Livermore National Laboratory under Contract No. W-7405-ENG-48.

¹D. L. Matthews *et al.*, Phys. Rev. Lett. **54**, 110 (1985).

²M. D. Rosen *et al.*, Phys. Rev. Lett. **54**, 106 (1985).

³M. H. Key, Nature **316**, 314 (1985).

⁴S. Suckewer *et al.*, Phys. Rev. Lett. **55**, 1753 (1985).

⁵O. Willi *et al.*, Proc. Soc. Photo-Opt. Instrum. Eng. **688**, 2 (1986).

⁶T. N. Lee, E. A. McLean, and R. C. Elton, Phys. Rev. Lett. **59**, 1185 (1987).

⁷S. Maxon *et al.*, J. Appl. Phys. **59**, 293 (1986).

⁸S. Maxon *et al.*, J. Appl. Phys. **57**, 971 (1985); **58**, 1706 (1985).

⁹B. MacGowan *et al.*, Phys. Rev. Lett. **59**, 2157 (1987).

¹⁰P. L. Hagelstein and S. Dalhed, Phys. Rev. A **37**, 1537 (1988).

¹¹J. P. Apruzese *et al.*, Phys. Rev. Lett. **55**, 1877 (1985).

¹²B. MacGowan *et al.*, J. Appl. Phys. **61**, 5243 (1987).

¹³M. D. Rosen *et al.*, Phys. Rev. Lett. **59**, 2283 (1987).

¹⁴See, for example, K. G. Whitney, J. Davis, and J. P. Apruzese, in *Cooperative Effects in Matter and Radiation*, edited by C. M. Bowden, D. W. Howgate, and H. R. Robl (Plenum, New York, 1977), p. 115.

¹⁵I. P. Grant *et al.*, Comput. Phys. Commun. **21**, 207 (1980).

¹⁶J. Reader and G. Luther, Phys. Rev. Lett. **45**, 609 (1980).

¹⁷G. B. Zimmerman, Lawrence Livermore National Laboratory Report No. UCRL-74811, 1973 (unpublished); P. D. Nielsen and G. B. Zimmerman, Lawrence Livermore National Laboratory Report No. UCRL-53123, 1981 (unpublished).

¹⁸P. L. Hagelstein, Ph.D. thesis, Massachusetts Institute of Technology, 1981; Lawrence Livermore National Laboratory Report No. UCRL-53100, 1981 (unpublished).

¹⁹P. L. Hagelstein, Phys. Rev. A **34**, 874 (1986).

²⁰P. Hagelstein and R. Jung, At. Data Nucl. Data Tables **37**, 121 (1987).

²¹M. H. Chen, Phys. Rev. A **35**, 4129 (1987).

²²P. L. Hagelstein, J. Phys. B **20**, 5785 (1987).

²³P. Hagelstein, M. Rosen, and V. Jacobs, Phys. Rev. **34**, 1931 (1986).

²⁴A. K. Burnham and G. T. Jameson, J. Vac. Sci. Technol. A **5**, 1713 (1987); G. D. Rambach and A. K. Burnham, Lawrence Livermore National Laboratory Report No. UCRL-94602, 1986 (unpublished).

²⁵J. Bailey *et al.*, Phys. Rev. A **35**, 2578 (1987).

²⁶P. Hagelstein and M. Runyan (unpublished).